J. Biochem. 131, 729–738 (2002)

Design, Production, and Characterization of Recombinant Neocarzinostatin Apoprotein in *Escherichia coli*[1]

Seishiro Nozaki,[*] Yoshihisa Tomioka,[*] Takanori Hishinuma,[*] Masayuki Inoue,[†] Yoko Nagumo,[†] Lilian R. Tsuruta,[*] Katsuhiro Hayashi,[*] Toshiki Matsumoto,[*] Yoshinori Kato,[*] Shunji Ishiwata,[*] Kunihiko Itoh,[‡] Toshio Suzuki,[‡] Masahiro Hirama,[†] and Michinao Mizugaki[*,2]

[*]*Department of Pharmaceutical Sciences, Tohoku University Hospital and Division of Clinical Pharmacy, Graduate School of Pharmaceutical Sciences, Tohoku University, 1-1 Seiryo-machi, Aoba-ku, Sendai, 980-8574;* [†]*Department of Chemistry, Graduate School of Science, Tohoku University, and CREST, Japan Science and Technology Corporation (JST), Aramaki-Aza-Aoba, Aoba-ku, Sendai, 980-8578; and* [‡]*Department of Pharmaceutical Sciences, Akita University Hospital, 1-1-1 Hondo, Akita 010*

Received February 28, 2002; accepted March 13, 2002

Neocarzinostatin (NCS) is the first discovered anti-tumor antibiotic having an enediyne-containing chromophore and an apoprotein with a 1:1 complex. An artificial gene library for NCS apoprotein (apo-NCS) production in *Escherichia coli* was designed and constructed on a phage-display vector, pJuFo. The recombinant phages expressing pre-apo-NCS protein were enriched with a mouse anti–apo-NCS monoclonal antibody, 1C7D4. The apo-NCS gene (*encsA*) for *E. coli* was successfully cloned, and then re-cloned into the pRSET A vector. After the his-tagged apo-NCS protein had been purified and cleaved with enterokinase, the binding properties of the recombinant protein as to ethidium bromide (EtBr) were studied by monitoring of total fluorescence intensity and fluorescence polarization with a BEACON 2000 system and GraphPad Prism software. A dissociation constant of 4.4 ± 0.3 μM was obtained for recombinant apo-NCS in the fluorescence polarization study. This suggests that fluorescence polarization monitoring with EtBr as a chromophore mimic may be a simplified method for the characterization of recombinant apo-NCS binding to the NCS chromophore. When Phe78 on apo-NCS was substituted with Trp78 by site-directed mutagenesis using a two stage megaprimer polymerase chain reaction, the association of the apo-NCS mutant and EtBr observed on fluorescence polarization analysis was of the same degree as in the case of the wild type, although the calculated maximum change (ΔIT_{max}) in total fluorescence intensity decreased from 113.9 to 31.3. It was suggested that an environmental change of the bound EtBr molecule on F78W might have dramatically occurred as compared with in the case of wild type apo-NCS. This combination of monitoring of fluorescence polarization and total fluorescence intensity will be applicable for determination and prediction of the ligand state bound or associated with the target protein. The histone-specific proteolytic activity was also re-investigated using this recombinant apo-NCS preparation, and calf thymus histone H1, H2A, H2B, H3, and H4. The recombinant apo-NCS does not act as a histone protease because a noticeable difference was not observed between the incubation mixtures with and without apo-NCS under our experimental conditions.

Key words: ethidium bromide, fluorescence polarization analysis, histone, megaprimer polymerase chain reaction, neocarzinostatin, phage display.

Neocarzinostatin (NCS) is one of the anti-tumor chromoprotein antibiotics isolated from culture filtrates of *Streptomyces carzinostaticus* var. F-41 (*S. carzinostaticus*) (*1*). NCS is composed of two components, an acidic single chain polypeptide (NCS apoprotein, apo-NCS) and a labile, nine-membered ring enediyne-containing chromophore (NCS-chr) in the molar ratio of 1:1 (*2–5*). Several enediyne antitumour agents have been isolated such as kedarcidin (*6–8*), and C-1027 (*9–11*), as nine-membered enediyne-containing choromoproteins, and maduropeptin (*12, 13*), esperamicin

[1]This work was supported by CREST, Japan Science and Technology Corporation (JST).
The nucleotide sequence in this study has been submitted to the DDBJ, EMBL, and GenBank nucleotide databases under accession numbers AB066225, AB066226, AB071856, AB071857, and AB071858.
[2]To whom correspondence should be addressed. Tel: +81-22-717-7525, Fax: +81-22-717-7545, E-mail: mizugaki@mail.cc.tohoku.ac.jp
Abbreviations: EtBr, ethidium bromide; FP, fluorescence polarization; IPTG, isopropyl-β-D-thiogalactopyranoside; IT, total fluorescence intensity; NCS, neocarzinostatin; apo-NCS, NCS apoprotein; NCS-chr, NCS chromophore; PFU, plaque forming unit; PAGE, polyacrylamide gel electrophoresis.

(*14*), calicheamicin (*15, 16*), and dynemicin (*17*), as ten-membered enediyne-containing compounds. On the first limited clinical evaluation of NCS, it was observed that NCS was effective for tumors resistant to other chemotherapeutics or radiation (*18*). In 1978, anti-tumor activity of NCS was detected in hepatomas and hematologic malignancies with an *iv* bolus daily for five times schedule, and in lung and colorectal carcinomas limitedly (*19*). In order to overcome the major problem and limitation regarding the clinical use of NCS, such as its severe toxicity and very short half-life ($t_{1/2}$), SMANCS (conjugate of NCS and poly (styrene-comaleic acid anhydride) was developed to make NCS more lipophilic and structurally stable (*20*). Therefore, apoproteins like apo-NCS remain excellent natural drug delivery systems.

The apoprotein part of chromoprotein is proposed to play at least two principle roles in the complex. Its primary role is as a packing carrier protein for the chemically unstable chromophore because apo-NCS strongly binds to and greatly stabilizes the labile chromophore (*21*). The secondary role of the apoprotein is as an enzyme exhibiting proteolytic activity toward basic proteins such as histones, which are most opposite in net charge to the highly acidic apoprotein (*13, 22*). These may allow a "targeted delivery" of the highly cytotoxic chromophore to the chromatin (*22*). A recent study showed that the potential proteolytic activities of apo-NCS may be very low (*23*).

It is known from X-ray and ^{1}H-NMR studies, that apo-NCS binds to a number of drugs including ethidium bromide (EtBr) and daunomycin (*24*). Therefore, fluorescence measurement of EtBr binding to apo-NCS is a convenient method for monitoring of the apo-NCS function. Fluorescence polarization (FP), the theory of which was first described by Perrin (*25*), is widely used for molecular interaction studies involving such as equilibrium binding assays (*26*), fluorescence polarization immuno-assay (FPIA) (*27*), DNA-protein interactions (*28*), or detection of single nuclear polymorphisms (*29, 30*). The polarization of a molecule is proportional to the molecule's rotational relaxation time, or the time it takes to rotate through an angle of 68.5°. The rotational relaxation time is related to viscosity (h), absolute temperature (T), molecular volume (V), and the gas constant (R). The polarization value (m) $\propto$ rotational relaxation time is proportional to $3hV/RT$. Therefore, if the viscosity and temperature are constant during an experiment, the polarization is directly proportional to the molecular volume. Changes in molecular volume result from the binding or dissociation of two molecules, degradation, or conformation changes (*26*).

In order to produce apo-NCS in *Escherichia coli*, we designed a synthetic DNA library for apo-NCS, and isolated the DNA coding apo-NCS for *E. coli* production using the phage display technique with an anti-NCS apoprotein monoclonal antibody. The recombinant protein and amino acid–substituted forms of it (positions Phe76 and Phe78) were over-expressed in *E. coli* BL21(DE3) and purified. The chromophore binding properties were studied and compared, using the fluorescence polarization method with ethidium bromide as a chromophore mimic.

EXPERIMENTAL PROCEDURES

Design of a Neocarzinostatin Apoprotein Gene for E. coli—To design apo-NCS for *E. coli*, we used the DNA sequence data under accession numbers D10996 and S65575 in the Gene Bank database, and checked the codon usage table of *E. coli* (http://www.dna.affrc.go.jp/~nakamura/CUTG.html) (*31*). Then we decided to use the optional codons for amino acids below in this study; Phe (UUU), Leu (CUG), Ile (AUY), Val (GUG), Ser (AGC), Pro (CCG), Thr (ACS), Ala (GCG), Tyr (UAU), Gln (CAG), Asn (AAY), Lys (AAA), Asp (GAU), Glu (GAA), Cys (UGY), Arg (CGY), and Gly (GGC). Then five restriction endonuclease sites, *Bgl*II (AGATCT), *Not*I (GCGGCCGCG), *Pst*I (CTGCAG), *Nhe*I (GCTAGC), and *Kpn*I (GGTACC), were designed, where code Y is base C or T; and code S is base G or C. The designed nucleotide sequence of apo-NCS for *E. coli*, named the *encsA* library, is shown in Fig. 2.

Design of a Template DNA Fragment Sequence for PCR Amplification—We designed five fragment libraries for DNA synthesis and PCR amplification from the *encsA* library. That is, N-I, 5′-GAAGA TCTAT GGTGC CGATY AGCAT YATYC GYAAY CGYGT GGCGA AAGTG GCGGT GGGCA GCGCG GCGGT GCTGG GCCTG GCGGT GGGCT TTCAG ACSCC GGCGG TGGCG GCCGC GCCGA-3′; N-II, 5′-AAGGA AAAAA GCGGC CGCGC CGACS GCGAC SGTGA CSCCG AGCAG CGGCC TGAGC GATGG CACSG TGGTG AAAGT GGCGG GCGCG GGCCT GCAGG CGGGC AC-3′; N-III, 5′-AAAAC TGCAG GCGGG CACSG CGTAT GATGT GGGCC AGTGY GCATG GGTGG ATACS GGCGT GCTGG CATGY AAYCC GGCGG ATTTT AGCAG CGTGA CSGCG GATGC GAAYG GCAGC GCTAG CAC-3; N-IV, 5′-CTAGC TAGCA CCAGC CTGAC SGTGC GYCGY AGCTT TGAAG GCTTT CTGTT TGATG GCACS CGYTG GGGCA CSGTG GATTG YACSA CSGCG GCATG CCA-3′; and N-V, 5′-ACATG CATGC CAGGT GGGCC TGAGC GATGC GGCGG GCAAY GGCCC GGAAG GCGTG GCGAT YAGCT TTAAY GGTAC CCC-3′. The nucleotide code used is the IUB-IUPAC standard.

Design of Primer Sets for PCR Amplification and Cloning—We designed primer sets for the PCR amplification of each DNA fragment. The ncs1 and ncs2 primers were used for the amplification of N-I; and the ncs3 and ncs4 primers, ncs5 and ncs6 primers, ncs7 and ncs8 primers, and ncs9 and ncs10 primers for N-II, N-III, N-IV, and N-V, respectively. The primer sequences were as follows: ncs1, 5′-GAAGATCTATGGTGC-3′; ncs2, 5′-GGGGTACCTCGGCGCGGCCGCCA-3′; ncs3, 5′-AAGGAAAAAAGCGGC-3′; ncs4, 5′-GGGGTACCGTGCCCGCCTG-3′; ncs5, 5′-AAAACTGCAGGCGGG-3′; ncs6, 5′-GGGGTACCGTGCTAGCGCTGCC-3′; ncs7, 5′-CTAGCTAGCACCAGCC-3'; ncs8, 5′-GGGGTACCTGGCATGCCGC-3′; ncs9, 5′-ACATGCATGCCAGGT-3′; and ncs10; 5′-GGGGTACCGTTAAAG-3′. The primers had the following restriction endonuclease sites for cloning, respectively: ncs1 (*Hin*dIII, *Bgl*II), ncs2 (*Kpn*I, *Not*I), ncs3 (*Not*I), ncs4 (*Kpn*I, *Pst*I), ncs5 (*Pst*I), ncs6 (*Kpn*I, *Nhe*I), ncs7 (*Nhe*I), ncs8 (*Kpn*I, *Sph*I), ncs9 (*Sph*I), and ncs10 (*Kpn*I).

Cloning of the apo-NCS Gene for E. coli—The *encsA* library was successively ligated and constructed on the pGEM-3Zf(+) phagemid DNA (Stratagene, La Jolla, CA, USA) by the PCR method using the above primers and template oligonucleotides. After this, the *encsA* library, named the pN-V library, on pGEM-3Zf(+) was digested with *Bgl*I and *Kpn*I, and its inserted DNA fragments were

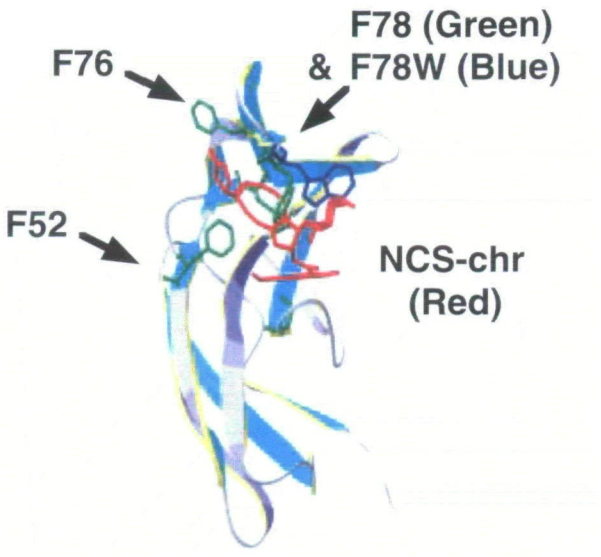

Fig. 1. **Protein modeling, and superimpositioning of apo-NCS and an amino substituted apo-NCS (F78W).** The positions of Phe52, Phe76, and Phe78 in apo-NCS are indicated by arrows. NCS-chr, Phe78, and Phe78Trp are colored red, green and blue, respectively.

ligated into the pJuFo vector, a phagemid for the display of cDNA libraries occurring on the phage surface (*32*). To enrich phages expressing the recombinant fos-apo-NCS, an antibody-panning procedure was performed with 1C7D4 mouse anti-NCS apoprotein monoclonal antibodies according to the standard instructions (*33*). Three rounds of panning were carried out in this study. *Bst*NI fingerprinting was performed to analyze clones obtained on panning for diversity. Some enriched phage clones were induced with isopropyl β-D-thiogalactopyranoside (IPTG) after culturing of transformed *E. coli* XL-1 Blue cells, and the cell lysates containing the recombinant apo-NCS were subjected to 12.5% SDS–polyacrylamide gel electrophoresis (PAGE) under reducing conditions with 2.5% of 2-mercaptoethanol and immunoblot analysis (*34*) using mAb 1C7D4.

DNA Sequencing—DNA sequencing was carried out with a Long-Read Tower DNA automated DNA sequencing system (Amersham Pharmacia Biotech, Tokyo). The sequencing primers were as follows: M13F, M13R, pJuFo-F (5′-CGCGAACCTGCTGAAAGAAA-3′), pJuFo-R (5′-GGCCAGTGAATTGTAATACGA-3′), RSETA-F (5′-CGCGAAATTAATACGACTCAC-3′), and RSETA-R (5′-GTTTAGAGGCCCCAAGGGGTTATG-3′). A Thermo Sequenase Cy5.0/Cy5.5 dye terminator sequencing kit (Amersham Pharmacia Biotech) was used for chemistry.

Construction of the Expression Vector of NCS Apoprotein in E. coli—Two primers were designed for expression of NCS apoprotein: ncsmF1 (5′-CGGGATCCGCCGCGCCGACCGCGACGGTGACCCCGAGC-3′) with a *Bam*HI site, and ncs_stop1R(5′-AATTCGGTACCCTAGTTAAAGCTGATCGCCACGCCTTCC-3′) with a *Kpn*I site and stop codon *tga*. PCR was performed using ncsmF1 and ncs_stop1R as primers, and pJuFo DNA obtained on panning as a template DNA. The PCR product was cloned into the pGEM-T easy vector (Promega) to give plasmid pR38. After pR38 DNA had been digested with *Bam*HI and *Kpn*I, the inserted DNA fragments were ligated into expression vector pRSET A (Invitrogen, San Diego, CA, USA) to give expression plasmid pR49. In this construct, the coding gene of the mature part of NCS apoprotein is fused to the polyhistidine metal binding domain and enterokinase cleavage site under the T7 RNA polymerase promoter. The *E. coli* strain used for expression was BL21(DE3)pLysS (Stratagene).

Purification of Recombinant apo-NCS—Cells freshly transformed with expression vector pR49 were grown on SB/carb+G medium (typically 10 ml) containing chloramphenicol (final concentration, 100 μg/ml) at 37°C overnight with shaking. The bacterial cells were pelleted by centrifugation and re-suspended in 10 ml fresh SB/carb to remove glucose, and then transferred to 100 ml of fresh SB medium (without glucose, carbenicillin, or chloramphenicol) and grown until an OD_{600} of 1.0 was attained. Then, IPTG, at a final concentration of 0.5 mM, was added to the culture, followed by further incubation for 4 h at 30°C with shaking. The bacterial cells were pelleted by centrifugation, and re-suspended in 5 ml of Bacterial Protein Extraction Reagent (B-PER®; Pierce, Rockford, IL, USA). To prepare a lysate, the suspension was sonicated ten times on ice with a TOMY Ultrasonic Disruptor Model VR 200P (TOMY Seiko, Tokyo) for two seconds at maximum power, and stored overnight at −20°C to allow it to freeze once. The next day, the bacterial cellular debris was removed by centrifugation, and the clear lysate was transferred to a clean tube.

Because the recombinant apo-NCS has the polyhistidine metal binding domain at its N-terminal, it was purified with a HiTrap chelating column (Amersham Pharmacia Biotech) charged with Ni^{2+}. Briefly, after equilibrating the HiTrap 1 ml column charged with Ni^{2+} with 10 ml of B-PER, 2.5 ml of a clear lysate was applied to the column, followed by washing with 10 ml of B-PER. Two step elution was then performed: the elution buffer for step 1 was 5 ml of 0.02 M sodium phosphate buffer (pH 7.4) containing 0.08 M imidazole and 0.125 M sodium chloride, and that for step 2 was 5 ml of 0.02 M sodium phosphate buffer (pH 7.4) containing 0.3 M imidazole and 0.125 M sodium chloride. The his-tagged recombinant apo-NCS was recovered on the step 2 elution. Each fraction was analyzed by SDS-PAGE. The purified protein was dialyzed against 0.02 M Tris-HCl (pH 8.0) containing 0.05 M sodium chloride and 0.002 M calcium chloride. One unit of enterokinase (Stratagene) per 150 μg of protein was added, followed by incubation for 17 h at 37°C. After enterokinase had been removed with STI agarose (Stratagene), the recombinant apo-NCS was subjected to Sephacryl S200 column (Amersham Pharmacia Biotech) chromatography with an FPLC system (Amersham Pharmacia Biotech) for further purification.

Site-Directed Mutation of NCS Apoprotein and Construction of Expression Vectors—Using a two stage megaprimer PCR method (*35, 36*), amino acid Phe78 of NCS apoprotein (apo-NCS) was mutated to Trp78 or Tyr78, and Phe76 to Trp76, respectively. The mutated primers (R49_F78Y, R49_F78, and R49_F76W) had the following sequences, respectively: R49_F78Y (5′-TTGAAGGCTTTCTGTATGATGGCACCCG-3′), T_m = 74.2°C, %GC = 50%, length = 28 bases; R49_F78W (5′-TTGAAGGCTTTCTGTGGGATGGCACCCG-3′), T_m = 78.8°C, %GC = 57.1%, length = 28 bases; and R49_F76W (5′-TTGAAGGCTGGCTGTTTGATGGCACCCG-3′), T_m = 79.7°C, %GC = 57.7%, length = 28 bases. The 5′-specific primer used was ncsmF1: ncsmF1 (5′-CGGGATC-

CGCCGCGCCGACCGCGACGGTGACCCCGAGC-3′), T_m = 98.2°C, %GC = 81.6%, length = 38 bases, and the 3′-specific primer used was ncs_stop1R: ncs_stop1R (5′-ATTCGGT-ACCCTAGTTAAAGCTGATCGCCACGCCTTCC-3′), T_m = 79.2°C, %GC = 51.3%, length = 39 bases. Each T_m value for the reaction mixture was calculated with Primer Express™ 1.5 software (PE Applied Biosystems Japan, Tokyo). The pR49 DNA was used as the PCR template.

Each PCR was performed with a GeneAmp PCR system model 2400 (PE Applied Biosystems Japan). Twenty-five-microliter PCR mixtures were set up for the first stage PCR. The composition of the reaction mixture was 10 mM Tris-HCl (pH 8.3), 50 mM KCl, 1.5 mM $MgCl_2$, 0.2 mM dGTP, 0.2 mM dATP, 0.2 mM dTTP, 0.2 mM dCTP, 1 mM mutated primer, 0.5 mM ncs_stop1R primer, 2.5 units TaKaRa Taq DNA polymerase, and 0.5 mM template pR49 DNA, with the following temperatures: denaturation at 94°C for 2 min; 20 cycles of 94°C for 30s, 60°C for 30s, 72°C for 60s. Then the second stage PCR was performed. Twenty-five-microliter PCR-premixes were set up. The composition of the reaction mixture was 10 mM Tris-HCl (pH 8.3), 50 mM KCl, 1.5 mM $MgCl_2$, 0.2 mM dGTP, 0.2 mM dATP, 0.2 mM dTTP, 0.2 mM dCTP, 2 mM ncsmF1 primer, and 2.5 units TaKaRa Taq DNA polymerase (Takara Shuzo Co., Otsu). Twenty-five microliters of each first stage PCR mixture was added to the second stage PCR mixture, followed by the second stage PCR at the following temperatures: denaturation at 94C for 2 min; 25 cycles of 94°C for 30s, 60°C for 30s, 72°C for 60s; and 72°C for 8 min.

DNA fragments were separated, excised, and purified from the agarose gel followed by cloning into the pGEM-T easy vector (Progega, Madison, WI, USA), respectively. After the insertion of the correct mutation had been confirmed by DNA sequencing, the fragments were opportunely digested and re-cloned into the pRSET A expression vector for *E. coli* (Invitrogen, San Diego, CA, USA), respectively. The recombinant clones, designated as p2S41/F76W, p2S45/F78Y, and p2S49/F78W, represented the expression vectors.

Histone-Cleavage Activity Measurement of PR49 Protein—Seven micrograms of the purified PR49 protein was incubated with 2 μg each of calf thymus histones H1, H2A, H2B, H3, and H4 (Roche Diagnostics, Tokyo) at 37°C for 12 h in 10 μl of 0.05 M Tris-HCl (pH 7.4). Next, the samples were heated in a Laemmli sample buffer for 1 min and then analyzed by SDS-PAGE (15% gel). The protein bands were visualized with GELCODE® Blue Stain Reagent (Pierce).

Ethidium Bromide Binding to apo-NCS with Fluorescence Polarization—Ethidium bromide (EtBr) binding to the recombinant apo-NCS was studied by fluorescence polarization with a Beacon 2000 fluorescence polarization system (PanVera, Madison, WI, USA) by monitoring the fluorescence polarization (*mP*) of an EtBr solution (λ_{ex} = 488 nm, λ_{em} = 617 nm) as a function of the recombinant apo-NCS concentration at 25°C. The emission filter of 617 nm (No. VP2400) was purchased from PanVera. Briefly, 120 μl of a reaction mixture containing 20 μl of BEACON™ BGG/phosphate buffer (pH 7.4; PanVera) and the purified recombinant apo-NCS at various concentrations was prepared in a disposable borosilicate glass tube (6 × 50 mm; PanVera). After measuring the background intensity, EtBr was added to a final concentration of 0.53 μM. After 10 min equilibration at 25°C, fluorescence polarization (*FP*) and total fluorescence intensity (*IT*) were measured in the three-cycle mode. Data were analyzed by using the sigmoidal dose-response model of non-linear regression in GraphPad Prism Ver 3.0a for Macintosh (GraphPad Software, San Diego, CA, USA), using the following equation: Y = Bottom +(Top + Bottom)/((1 + 10^((logK_d–X)*Hill slope)), where X is the logarithm of the apo-NCS concentration (*M*), and Y is each response for *IT* or mP; bottom is the baseline response of IT_{min} or mP_{min}, top is the maximum response of IT_{max} or mP_{max}, and K_d is the dissociation constant.

Protein Modeling—Protein modeling of apo-NCS with Phe78 substituted to Trp78 was performed using SWISS-MODEL, a free Automated Protein Modeling Server version 3.5 on the Internet (http://www.expasy.ch/swissmod/) written by Peitsch (*37, 38*). The templates for modeling used were PDB (the Protein Data Bank) entry 1NOA.pdb, 1NCO.pdb, 2MCM.pdb, and 1HZK.pdb. Models were visualized and outputted with Swiss-Pdb Viewer (Deep View) (*39*).

RESULTS

Library Construction and Screening of apo-NCS for E. coli—A set of preferred codons for *E. coli* (*31*) was used to design a nucleotide library for apo-NCS for *E. coli*, because the substitution of rare codons with optimal ones affects not only the rate of elongation but also mRNA stability and initiation. A total of 31 amino acids—4 Ile (ATY), 14 Thr (ACS), 5 Asn (AAY), 5 Arg (CGY), and 3 Cys (TGY)— were designed as mixed codons, respectively (Fig. 2). The resulting fos-fused NCS apoprotein (fos-apo-NCS) library (titer, 10^{11} CFU/ml) associated with the Jun-decorated phage particles was incubated with a plate coated with an anti–apo-NCS monoclonal antibody (1C7D4) to enrich the recombinant phages expressing fos-apo-NCS, non-specific binding phages being removed by washing and bound phages being eluted with acid. After three rounds of panning procedures, five phagemid DNA clones were subjected to Western blot analysis using 1C7D4 mAb to confirm (Fig. 3). Four (80%) of the five samples expressed fos-apo-NCS of approximately 23 kDa (Fig. 3, lanes 2–5). These four phagemids also have *Not*I, *Pst*I, *Nhe*I, and *Sph*I restriction endonuclease sites in the inserted DNA, as expected.

DNA Sequence Encoding apo-NCS for E. coli—The four clones obtained were subjected to DNA sequence analyses. Unfortunately, we could not obtain the first planned gene full-encoding apo-NCS precursor because they had the same mutation in their nucleotide sequences. A pN72 (accession number, AB066225) had three additional G (bold characters, G50, G54, and G103) in the signal peptide region of apo-NCS, and then a frame shift occurred. Consequently, the selected codons of 24 amino acids designed as mixed codons in the mature encoding region were 1 Ile (ATC), 13 Thr (6 ACC, 7 ACG), 4 Asn (2 AAT, 2 AAC), 3 Arg (3 CGC), and 3 Cys (2 TGC, 1 TGT), the exceptions being 6 amino acids (3 Ile, 1 Asn, and 2 Arg) in the signal peptide region. The base content of 339 base pairs for 113 amino acids was 136 G, 56 A, 54 T, and 93 C, but 121 G, 40 A, 54 T, and 124 C for *ncsA*. Its %GC was 67.6% as compared with 72.3% of *ncsA* (Fig. 4).

Expression of apo-NCS in E. coli—We decided to use this

```
                11          20          29          38          47          56
5'  CAA GCT TGA AGA TCT ATG GTG CCG ATY AGC ATY ATY CGY AAY CGY GTG GCG AAA
    --- --- --- --- --- --- --- --- --- --- --- --- --- --- --- --- --- ---
                        M   V   P   I   S   I   I   R   N   R   V   A   K

                65          74          83          92         101         110
    GTG GCG GTG GGC AGC GCG GCG GTG CTG GGC CTG GCG GTG GGC TTT CAG ACS CCG
    --- --- --- --- --- --- --- --- --- --- --- --- --- --- --- --- --- ---
     V   A   V   G   S   A   A   V   L   G   L   A   V   G   F   Q   T   P

               119         128         137         146         155         164
    GCG GTG GCG GCC GCG CCG ACS GCG ACS GTG ACS CCG AGC AGC GGC CTG AGC GAT
    --- --- --- --- --- --- --- --- --- --- --- --- --- --- --- --- --- ---
     A   V   A   A   A   P   T   A   T   V   T   P   S   S   G   L   S   D

               173         182         191         200         209         218
    GGC ACS GTG GTG AAA GTG GCG GGC GCG GGC CTG CAG GCG GGC ACS GCG TAT GAT
    --- --- --- --- --- --- --- --- --- --- --- --- --- --- --- --- --- ---
     G   T   V   V   K   V   A   G   A   G   L   Q   A   G   T   A   Y   D

               227         236         245         254         263         272
    GTG GGC CAG TGY GCA TGG GTG GAT ACS GGC GTG CTG GCA TGY AAY CCG GCG GAT
    --- --- --- --- --- --- --- --- --- --- --- --- --- --- --- --- --- ---
     V   G   Q   C   A   W   V   D   T   G   V   L   A   C   N   P   A   D

               281         290         299         308         317         326
    TTT AGC AGC GTG ACS GCG GAT GCG AAY GGC AGC GCT AGC ACS AGC CTG ACS GTG
    --- --- --- --- --- --- --- --- --- --- --- --- --- --- --- --- --- ---
     F   S   S   V   T   A   D   A   N   G   S   A   S   T   S   L   T   V

               335         344         353         362         371         380
    CGY CGY AGC TTT GAA GGC TTT CTG TTT GAT GGC ACS CGY TGG GGC ACS GTG GAT
    --- --- --- --- --- --- --- --- --- --- --- --- --- --- --- --- --- ---
     R   R   S   F   E   G   F   L   F   D   G   T   R   W   G   T   V   D

               389         398         407         416         425         434
    TGY ACS ACS GCG GCA TGC CAG GTG GGC CTG AGC GAT GCG GCG GGC AAY GGC CCG
    --- --- --- --- --- --- --- --- --- --- --- --- --- --- --- --- --- ---
     C   T   T   A   A   C   Q   V   G   L   S   D   A   A   G   N   G   P

               443         452         461
    GAA GGC GTG GCG ATY AGC TTT AAY GGT ACC CC 3'
    --- --- --- --- --- --- --- --- --- --- --
     E   G   V   A   I   S   F   N
```

Fig. 2. **Design of the apo-NCS gene and the derived amino-acid sequence for *E. coli*.** The nucleotide code used is the IUB-IUPAC standard.

pN72 DNA for recombinant apo-NCS production without further screening, and performed a sub-cloning of the mature gene encoding apo-NCS into *E. coli* expression vector pRSET A. Primers were designed for PCR, with a *Bam*HI site for the forward primer (ncsmF1), and a *Kpn*I site and stop codon TAG for the reverse primer (ncs_stop1R), as described in "EXPERIMENTAL PROCEDORES." The expression vector pR49/pRSET A DNA for apo-NCS was successfully prepared. In this construct, the coding gene of the mature part of apo-NCS is fused to the polyhistidine metal binding domain and enterokinase cleavage site under the T7 RNA polymerase promoter. *E. coli* BL21(DE3) pLysS was transformed with pR49 DNA for the expression of 6× His-tagged apo-NCS. At 37°C, some of the expressed protein was associated with the cell lysate pellet, but the yield of soluble protein increased at 30°C. The time of induction with 0.5 mM IPTG was four hours. The average weight of cultured *E. coli* cells was 1.1 g per 100 ml of SB medium culture. *E. coli* lysates in the B-PER were then subjected to HiTrap Chelating affinity column chromatography with two-step elution with 0.08 and 0.3 M imidazole. The metal ion used was Ni^{2+}. The purified protein of 15.2 kDa was homogeneously eluted with 0.3 M imidazole (Fig. 5a, lane 5). The yield of recombinant His-tagged apo-NCS (PR49) was approximately 0.45 mg/g of *E. coli* cells (4 mg recombinant protein/liter culture). The purified PR49 protein was treated with enterokinase to obtain the apo-NCS, named PR49EK, with a cleaved N-terminal extra-peptide. As shown in Fig. 4b, SDS-PAGE analysis showed the cleavage of PR49 (149 amino acids residues) of 15.2 kDa into PR49EK (118 amino acid residues) of 11.7 kDa and the leader peptide (31 amino acid residues) of 3.5 kDa. This PR49EK would have the DRWGS sequence of 5 amino acid residues of 619.9 Da in the N-terminal of the native apo-NCS (113 amino acid residues). Moreover, the recombinant protein yields from 400 ml cultures were 5.31 mg/3.8 g of *E. coli* for F76W (P2S41), 1.30 mg/1.6 g of *E. coli* for F78Y (P2S45), and 4.4 mg/4.2 g of *E. coli* for F78W (P2S49). SDS-

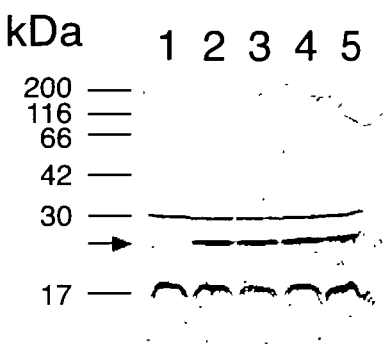

Fig. 3. **Western blot analysis of an *E. coli* lysate expressing the Fos-NCS apoprotein fusion protein using anti-apo-NCS monoclonal antibodies.** *E. coli* lysate samples were separated by SDS-PAGE (12.5% gel) under reducing conditions, and then transferred to a nitrocellulose membrane. Western blot analysis was performed with anti-apo-NCS monoclonal antibody 1C7D4, and development with a DAB-hydroperoxide system. The samples were *E. coli* lysates transformed with pJuFo-derived vector DNA of pN51 (lane 1), pN69 (lane 2), pN72 (lane 3), pN75 (lane 4), and pN80 (lane 5). The molecular weights of markers are indicated on the left in kilodaltons. The solid arrow indicates the mobility of the Fos-apo-NCS fusion protein of 23 kDa.

PAGE analysis revealed only one band with same electrophoretic mobility for the mutant and wild type proteins (data not shown).

Ethidium Bromide Binding to the Recombinant apo-NCS (PR49EK) and Mutants—It is convenient for fluorescence measurement to monitor the ethidium bromide (EtBr)-binding function as to apo-NCS because it has been shown that EtBr binds to the natural and recombinant apo-NCS in the same vicinity of the cleft (*23, 24*). Therefore, the changes in total fluorescence intensity and fluorescence polarization (FP) were observed as a function of added total recombinant apo-NCS (Fig. 6). No fluorescence intensity was measured in the absence of EtBr when λ_{ex}=488 nm and λ_{em}=617 nm (data not shown). The maximum change in fluorescence (ΔIT_{max}) was calculated to be 113.9 for the wild type recombinant apo-NCS. The observed dissociation constant (K_d) was 14.4 μM (95% confidence interval value, 13.1 to 15.8 μM). On FP analysis, the K_d was calculated to be 4.39 μM (95% confidence interval value, 4.2 to 4.7 μM) with 155.0 millipolarization units (mPU; 1 PU = 1,000 mPU) of the maximum change of FP (ΔFP_{max}) and 0.92 of the Hill slope value (Fig. 6A). The effects of amino acid substitutions of apo-NCS on EtBr binding were also investigated. Each maximum and minimum value of *FP* was calculated, as shown in Table I. The ΔFP_{max} values were 153.3 mPU for

```
                        10        20        30        40        50
ncsA          1 GCGGCGCCGACGGCTACGGTGACTCCGTCGTCCGGTCTGTCCGACGGCAC    50
                A  A  P  T  A  T  V  T  P  S  S  G  L  S  D  G  T
pN72m         1 ..C........C..G........C...AGCAG...C...AG...T.....    50

                        60        70        80        90       100
ncsA         51 CGTGGTCAAGGTCGCCGGCGCGGGTCTCCAGGCCGGAACGGCCTACGACG   100
                 V  V  K  V  A  G  A  G  L  Q  A  G  T  A  Y  D  V
pN72m        51 G.....G..A..G..G........C..G.....G..C..C..G..T..T.    100
                                          Pst I

                       110       120       130       140       150
ncsA        101 TCGGGCAGTGCGCGTGGGTGGACACCGGTGTTCTCGCGTGCAACCCGGCG   150
                  G  Q  C  A  W  V  D  T  G  V  L  A  C  N  P  A
pN72m       101 .G..C..A.....A........T..G..C..G..G..A..T.........   150

                       160       170       180       190       200
ncsA        151 GACTTCTCCTCCGTGACCGCGGACGCCAACGGCTCCGCGAGCACGTCGCT   200
                 D  F  S  S  V  T  A  D  A  N  G  S  A  S  T  S  L
pN72m       151 ..T..TAG.AG............T..G..T...AG...T.....CAGC..   200
                              Sac II                 Nhe I

                       210       220       230       240       250
ncsA        201 GACGGTGCGCCGCTCCTTCGAGGGCTTCCTCTTCGACGGCACCCGCTGGG   250
                  T  V  R  R  S  F  E  G  F  L  F  D  G  T  R  W  G
pN72m       201 .............AG...T..A.....T..G..T..T.............   250

                       260       270       280       290       300
ncsA        251 GCACCGTGGACTGCACCACCGCGGCCTGCCAGGTCGGCCTCTCGGACGCT   300
                   T  V  D  C  T  T  A  A  C  Q  V  G  L  S  D  A
pN72m       251 ....G.....T.....G..G.....A........G.....GAGC..T..G   300
                                          Sph I

                       310       320       330       340       350
ncsA        301 GCGGGCAACGGCCCGGAGGGTGTGGCGATCTCCTTCAAC             350
                 A  G  N  G  P  E  G  V  A  I  S  F  N
pN72m       301 ........T........A..C.........AG...T...             350
```

Fig. 4. **Nucleotide sequence comparison between *ncsA* and pN72m (*encsA*) with the predicted amino acid sequence of the encoded protein.** The nucleotide sequences of the mature NCS apoprotein coding region of *ncsA* from *S. neocarzinostaticus* and pN72 from *E. coli* are shown in the top and bottom lines of each row with a restriction endonuclease cleavage site for the pN72 sequence (identical residues are indicated by dots in the pN72m sequence). Nucleotides are numbered beginning with the first Ala.

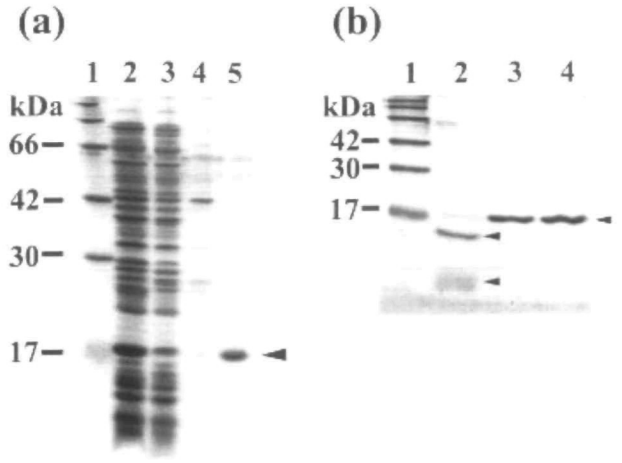

Fig. 5. **SDS-PAGE of recombinant apo-NCS purified from *E. coli* transformed with pR49.** (a) SDS-PAGE analysis (12.5% gel) at different steps of purification of the expressed His-tagged apo-NCS (PR49). Lane 1, standards protein markers. The molecular weights of markers are indicated on the left (in kilodaltons). The samples were: *E. coli* lysate transformed with pR49/pRSET A in the B-PER (lane 2); pass-through fraction on nickel chelating column chromatography (lane 3); fraction eluted with 0.08 M imidazole in 0.02 M phosphate buffer, pH 7.4, containing 0.125 M NaCl (lane 4); and fraction eluted with 0.3 M imidazole in 0.02 M phosphate buffer, pH 7.4, containing 0.125 M NaCl (lane 5). The solid triangle indicates the mobility of the PR49 protein expressed in *E. coli*. (b) SDS-PAGE analysis of enterokinase treatment of the PR49 protein. Lane 1, standards protein markers. The samples, 1.5 μg protein per lane, were: PR49 protein with 17 h incubation at 37°C in 0.02 M Tris-HCl (pH 8.0) containing 0.05 M NaCl and 0.002 M $CaCl_2$ with (lane 2) or without (lane 3) one unit of enterokinase, and PR49 protein without incubation (lane 4). The solid triangles indicate the mobility of PR49 (top), PR49EK (middle), and the leader peptide cleaved (bottom), respectively.

F78Y, 197.0 mPU for F78W, and 153.3 mPU for F76W, respectively. The ΔFP_{max} value for the F78W mutant was higher than those for the wild type and other recombinant proteins. As shown in Table III, the K_d values between EtBr and each apo-NCS in the FP study were calculated from fitting curves to be 2.77 mM for the F78Y mutant, 5.16 μM for the F78W mutant, and 2.77 μM for the F76W mutant, respectively. On the other hand, a major increase in IT as a function of the recombinant apo-NCS concentration was not observed only for the F78W mutant as compared with in the cases of the wild type, F78Y mutant and F76W mutant (Fig. 6, B, D, F, and H). As shown in Table II, the ΔIT_{max} under this condition was calculated to be 112.6 for F78Y, 31.3 for F78W, and 120.3 for F76W, respectively. It was also predicted that there was a single class of EtBr binding site (1:1 complex of apo-NCS and EtBr) in the each recombinant apo-NCS because the Hill slope values calculated were approximately 1.0 from on both FP analysis and IT analysis (Table III), respectively. These results indicated that each mutant apo-NCS protein (F76W, F78Y, and F78W) associated with EtBr under this experimental condition. The decrease of the IT change in the F78W mutant might not be due to the non-binding of F78W to EtBr.

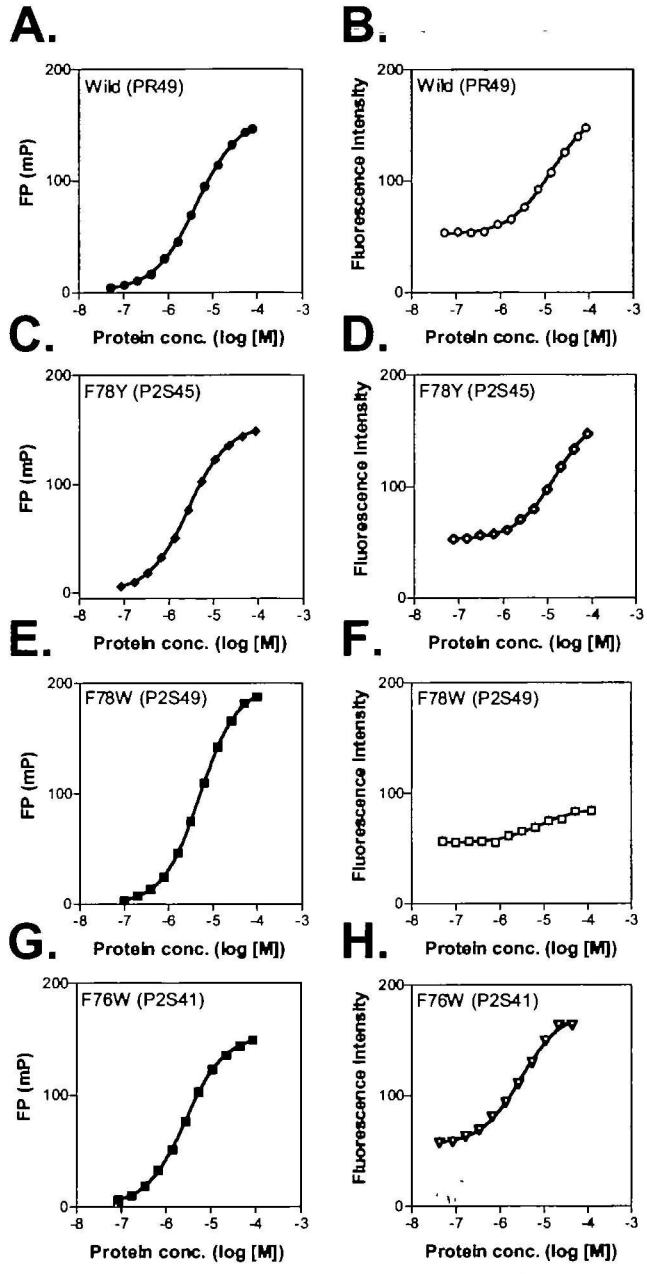

Fig. 6. **Equilibrium binding isotherm of recombinant apo-NCS and mutant proteins as to EtBr.** losed symbols (A, C, E, and G) represent the isotherm of the fluorescence polarization (*mP*) at each titration point as a function of the total recombinant apo-NCS concentration added to the binding reaction of 0.53 μM EtBr. Open symbols (B, D, F, and H) represent the isotherm of the total fluorescence intensity. Actual data points and a computer-fitting curve obtained using the sigmoidal dose-response model of non-linier regression in GraphPad Prism Ver3.0a for Machintosh are shown, respectively. ● and ○, PR49EK (wild); ◆ and ◇, P2S45EK (F78Y); ■ and □, P2S49EK (F78W); ▼ and ▽, P2S41EK (F76W).

Re-Examination of Histone-Cleavage Activities of the PR49 and PR49EK Proteins—To estimate the proteolytic activities of the PR49 and PR49EK proteins, calf thymus histones H1, H2A, H2B, H3, and H4 were each incubated either with or without purified PR49 protein (Fig. 7a) or PR49EK protein (Fig. 7b). However, a noticeable difference

TABLE I. **Calculated maximum and minimum values of fluorescence polarization.**

	FP_{max}	FP_{min}	ΔFP_{max}
Wild	156.8 ± 1.5	1.8 ± 0.9	155.0
F78Y	153.3 ± 1.0	1.3 ± 1.0	152.0
F78W	197.0 ± 1.0	0.4 ± 0.7	196.6
F76W	153.3 ± 1.0	1.3 ± 1.3	152.0

Data are represented as millipolarization units (mPU).

TABLE II. **Calculated maximum and minimum values of total fluorescence intensity.**

	IT_{max}	IT_{min}	ΔIT_{max}
Wild	165.9 ± 2.0	52.0 ± 0.4	113.9
F78Y	165.0 ± 2.0	52.4 ± 0.5	112.6
F78W	86.3 ± 2.9	55.0 ± 0.7	31.3
F76W	175.7 ± 2.2	55.4 ± 1.1	120.3

TABLE III. **Observed equilibrium dissociation constants for EtBr and each recombinant apo-NCS.**

Parameter	Observed equilibrium dissociation constant (μM)	95% Confidence interval (μM)	Hill slope
Fluorescence polarization			
Wild	4.39	4.15–4.65	0.92
F78Y	2.77	2.64–2.90	0.99
F78W	5.16	5.00–5.32	1.04
F76W	2.77	2.64–2.90	0.99
Total fluorescence intensity			
Wild	14.4	13.1–15.8	0.91
F78Y	14.9	13.8–16.2	0.99
F78W	7.81	6.05–10.0	0.97
F76W	3.08	2.78–3.42	0.94

was not observed in the incubation mixture between with and without PR49 or PR49EK under our experimental conditions (Fig. 7).

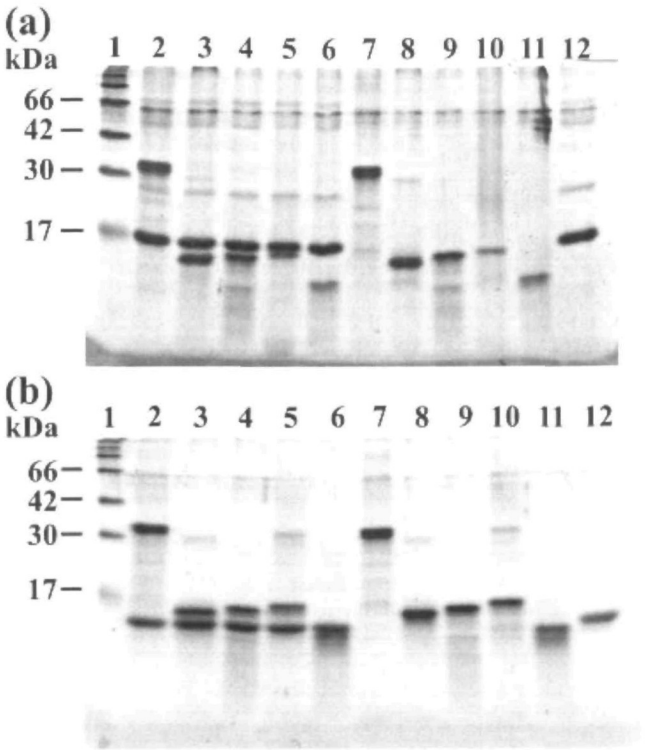

Fig. 7. **SDS-PAGE analysis of the reaction of PR49 and PR49EK(apo-NCS) protein with calf thymus histone.** (a) Seven micrograms of the purified PR49 protein (a) or 5.4 μg of the purified PR49EK protein (b) were incubated with 2 μg each of calf thymus histones H1, H2A, H2B, H3, and H4 (Roche Diagnostics, Tokyo) at 37°C for 12 h in 10 μl of 0.05 M Tris-HCl (pH 7.4). After the addition of 10 μl of a Laemili sample buffer, the samples were heated and analyzed by SDS-PAGE (15% gel). Lanes 2, 3, 4, 5, and 6, reactions of the PR49 (a) or PR49EK protein (b) with H1, H2A, H2B, H3, and H4, respectively; lanes 7, 8, 9, 10, and 11, control reactions with H1, H2A, H2B, H3, and H4, respectively; lane 12, control reaction with just PR49 (a) or PR49EK (b) protein; lane 1, standards protein markers. The molecular weights of markers are indicated on the left in kDa.

DISCUSSION

In this paper, the binding properties of EtBr, as a chromophore mimic, as to recombinant apo-NCS or amino acid-substituted apo-NCS mutants are reported. It is generally well known that EtBr, a cationic dye, interacts strongly and specifically with double helical RNAs and DNAs, and is widely used in spectrofluorimetric analyses with striking fluorescence enhancement. It is generally agreed that strong fluorescence enhancement accompanies intercalation of EtBr into the double helix conformation of nucleic acids. The low intensity of free EtBr in water is attributed to efficient quenching of excited state molecules by proton transfer to water molecules, and the enhancement of the fluorescence intensity on binding to nucleic acids is attributed to a reduction in the proton transfer rate (*40*). The mechanism suggests that the fluorescence quantum yield differs with the degree of exposure to the solvent of the intercalated EtBr molecules.

It is known from X-ray and ^{1}H-NMR studies that apo-NCS binds to a number of drugs including ethidium bromide (EtBr) and daunomycin (*24*). EtBr has been used as a chromophore mimic and a fluorescence tracer, because it also might be sandwiched by Phe52, Phe78, and the Cyst37–Cys47 disulfide bond (*24*). NCS-chr is tightly and non-covalently bound to apo-NCS, because the dissociation constant (K_d) of the biologically active chromophore is approximately 0.1 nM (*41*). On the other hand, the K_d values for the ethidium-NCS complex were 0.857 μM natural apo-NCS (*24*), 1 μM natural apo-NCS, and 2 μM recombinant apo-NCS (*23*), as judged on fluorescence measurement, and 4.4 μM recombinant apo-NCS, as found in this fluorescence polarization study. These data indicate that the recombinant apo-NCS obtained in this study may have a binding function as apo-NCS. It was suggested that the monitoring of fluorescence polarization using EtBr may be a useful way of characterizing recombinant apo-NCS binding to NCS-chr.

Site-directed mutagenesis involving a two stage megaprimer PCR (*35, 36*) was carried out to investigate the functional roles of amino acid residues of apo-NCS in the chromophore-binding cleft. Mutant apo-NCS possessing amino acid substitutions were produced with attention to the positions at which residues are expected to be involved in the binding with the chromophore based on X-ray crystallographic studies (*21, 42*) and NMR spectroscopic structural analyses (*43–47*). Moreover, Mohanty *et al.* demon-

strated the amino acid residues that are involved in the binding of EtBr and apo-NCS at amino acid residues (*24*). At first, two positions, Phe76 and Phe78 in apo-NCS, were selected for substitution to another aromatic group (Fig. 1). Each recombinant apo-NCS mutant (F78Y, F78W, and F76W) could be successfully obtained from an *E. coli* culture.

When Phe78 was substituted with Trp78, the association of apo-NCS and EtBr observed was the same as in the case of the wild type apo-NCS, as judged from the results of FP analysis (Fig. 6). The calculated ΔFP_{max} value for the F78W mutant seemed to be higher than those for other recombinant apo-NCS, as shown in Table I. This suggested that EtBr could bind the F78W mutant with a single EtBr binding site, and that a change in molecular volume including a conformation change had obviously occurred in F78W as compared with in other proteins. Therefore, the decrease in the calculated ΔIT_{max} value for F78W as compared with the wild type apo-NCS was an indication of an environmental change of the bound EtBr molecule on F78W. The functional roles of the Phe78 residue on apo-NCS are thought to be molecular cap holding of the NCS-chr π-face tightly in cooperation with Phe52, and the formation of a hydrophobic environment to protect the labile chromophore (*21*). Therefore, the bound EtBr in the F78W mutant may be more solvent-exposed than in the case of the wild type, F78Y, or F76W; that is, a molecular cap of Trp78 may slip off the bound EtBr, as modeled and shown in Fig. 1, resulting in the formation of an insufficient hydrophobic environment. Alternatively, it could be interpreted that the affinity of the F78W mutant to EtBr is weaker than those of others because the K_d value was 5.2 μM for F78W. One possibility is that the structure of F78W is destabilized. Anyway, these results indicate that Phe78 on apo-NCS is a more important amino acid residue than Phe76 for the wrapping of the choromophore to form an hydrophobic environment, it being shown previously that the hydrophobic interaction between NCS-chr and apo-NCS is important (*48*). The future direction for clarifying the effects of amino acid substitutions for apo-NCS should be X-ray and ^{1}H-NMR analysis of apo-NCS mutants.

It is unclear why differences between the K_d values determined in each *FP* and *IT* experiment were observed, especially for the recombinant wild type apo-NCS and F78Y mutant. Because the slope of the Hill plot was approximately 1, which indicates that there is a single class of binding site as to EtBr and apo-NCS, one speculation is that these differences may be due to the states (the binding properties) of the EtBr and apo-NCS interaction. Although further investigations should be conducted carefully, the data obtained in the IT experiment may express the packing properties, and those in the FP one may express the binding properties including the packed state of EtBr as to apo-NCS, respectively.

The proteolytic activity of apo-NCS toward histones (especially histone H1), which is associated with the DNA cleavage activity by the NCS chromophore, reflcets the potential appearance of a new protease family because a highly acidic protein such as apo-NCS would probably interact with highly basic proteins such as histones. However, a recent study involving a recombinant apo-NCS produced by *E. coli* also showed that this proteolytic activity toward histones or synthetic peptides can be physically separated from the apoprotein (*23*). Our preparation of this recombinant apo-NCS, although it has DRWGS as N-terminal extra 5 amino acid residues, does not exhibit histone-cleavage activity. Our data strongly agree with their observation that apo-NCS does not exhibit proteolytic activity toward histones.

Tsunoda *et al.* demonstrated that the immunoconjugate of anti-tumor vascular endothelium monoclonal antibodies (TES-23) and NCS would be a useful drug carrier complex with high specificity to tumors and effects on tumor regression in rats bearing KMT-17 fibrosarcomas (*49*). Therefore, the direct modification of apo-NCS with some targeting molecule might be more effective for clinical needs.

Protein engineering has unlimited potential as to significant advances in science, medicine and industry (*50*). One of the major goals of such approaches is the design, modification and production of proteins with improved protein properties, such as molecular recognition, stability, safety, *etc.*, that have new functions not found in nature. The ability to tailor-make a protein with a predetermined function and structure is the ultimate dream.

We are grateful to Dr. Crameri for the generous gift of pJuFo DNA. YT thanks Dr. Randy Buck and Vanessa Buck for reviewing this manuscript.

REFERENCES

1. Ishida, N., Miyazaki, K., Kumagai, K., and Rikimaru, M. (1965) Neocarzinostatin, an antitumor antibiotic of high molecular weight: isolation, physiochemical properties and biological activities. *J. Antibiotics Ser. A* **18**, 68–76
2. Napier, M.A., Holmquist, B., Strydom, D.J., and Goldberg, I.H. (1979) Neocarzinostatin: Spectral characterization and separation of a non-protein chromophore. *Biochem. Biophys. Res. Commun.* **89**, 635–642
3. Koide, Y., Ishii, F., Hasuda, K., Koyama, Y., Edo, K., Katamine, S., Kitame, F., and Ishida, N. (1980) Isolation of a non-protein component and a protein component from neocarzinostatin (NCS) and their biological activities. *J. Antibiot.* **33**, 342–346
4. Edo, K., Mizugaki, M., Koide, Y., Seto, H., Furihara, K., Otake, N., and Ishida, N. (1985) The structure of neocarzinostatin chromophore processing a novel bicyclo[7,3,0]dodecadiyne system. *Tetrahedron Lett.* **26**, 331–334
5. Edo, K., Akiyama, Y., Saito, K., Mizugaki, M., Koide, Y., and Ishida, N. (1986) Absolute configuration of the amino sugar moiety of the neocarzinostatin chromophore. *J. Antibiot. (Tokyo)* **39**, 1615–1619
6. Lam, K.S., Hesler, G.A., Gustavson, D.R., Crosswell, A.R., Veitch, J.M., and Forenza, S. (1991) Kedar cidin, a new chromoprotein antitumor antibiotic. 1. Taxonomy of producing organism, fermentation and biological-activity. *J. Antibiot.* **44**, 472–478
7. Hofstead, S.J., Matson, J.A., Malacko, A.R., and Marquardt, H. (1992) Kedarcidin, a new chromoprotein antitumor antibiotic. II. Isolation, purification and physico-chemical properties. *J. Antibiot. (Tokyo)* **45**, 1250–1254
8. Zein, N., Colson, K.L., Leet, J.E., Schroeder, D.R., Solomon, W., Doyle, T.W. and Casazza, A.M. (1993) Kedarcidin chromophore: an enediyne that cleaves DNA in a sequence- specific manner. *Proc. Natl. Acad. Sci. USA* **90**, 2822–2826
9. Otani, T., Minami, Y., Marunaka, T., Zhang, R., and Xie, M.Y. (1988) A new macromolecular antitumor antibiotic, C-1027. II. Isolation and physico-chemical properties. *J. Antibiot. (Tokyo)* **41**, 1580–1585
10. Sugiura, Y. and Matsumoto, T. (1993) Some characteristics of DNA strand scission by macromolecular antitumor antibiotic C-1027 containing a novel enediyne chromophore. *Biochemistry*

32, 5548–5553
11. Xu, Y.J., Zhen, Y.S., and Goldberg, I.H. (1994) C1027 chromophore, a potent new enediyne antitumor antibiotic, induces sequence-specific double-strand DNA cleavage. *Biochemistry* **33**, 5947–5954
12. Hanada, M., Ohkuma, H., Yonemoto, T., Tomita, K., Ohbayashi, M., Kamei, H., Miyaki, T., Konishi, M., Kawaguchi, H., and Forenza, S. (1991) Maduropeptin, a complex of new macromolecular antitumor antibiotics. *J. Antibiot. (Tokyo)* **44**, 403–414
13. Zein, N., Solomon, W., Colson, K.L., and Schroeder, D.R. (1995) Maduropeptin: an antitumor chromoprotein with selective protease activity and DNA cleaving properties. *Biochemistry* **34**, 11591–11597
14. Sugiura, Y., Uesawa, Y., Takahashi, Y., Kuwahara, J., Golik, J., and Doyle, T.W. (1989) Nucleotide-specific cleavage and minor-groove interaction of DNA with esperamicin antitumor antibiotics. *Proc. Natl. Acad. Sci. USA* **86**, 7672–7676
15. Yu, L., Goldberg, I.H., and Dedon, P.C. (1994) Enediyne-mediated DNA damage in nuclei is modulated at the level of the nucleosome. *J. Biol. Chem.* **269**, 4144–4151
16. Thorson, J.S., Sievers, E.L., Ahlert, J., Shepard, E., Whitwam, R.E., Onwueme, K.C., and Ruppen, M. (2000) Understanding and exploiting nature's chemical arsenal: the past, present and future of calicheamicin research. *Curr. Pharm. Des.* **6**, 1841–1879
17. Sugiura, Y., Shiraki, T., Konishi, M., and Oki, T. (1990) DNA intercalation and cleavage of an antitumor antibiotic dynemicin that contains anthracycline and enediyne cores. *Proc. Nat.l Acad. Sci. USA* **87**, 3831–3835
18. Takahashi, M., Toriyama, K., Maeda, H., Kikuchi, M., and Kumagai, K. (1969) Clinical trials of a new antitumor polypeptide: neocarzinostatin (NCS). *Tohoku J. Exp. Med.* **98**, 273–280
19. Griffin, T.W., Comis, R.L., Lokichi, J.J., Blum, R.H., and Canellos, G.P. (1978) Phase I and preliminary phase II study of neocarzinostatin. *Cancer Treat. Rep.* **62**, 2019–2025
20. Maeda, H. (2001) SMANCS and polymer-conjugated macromolecular drugs: advantage in cancer chemotherapy. *Adv. Drug Delivery Rev.* **46**, 169–185
21. Kim, K.H., Kwon, B.M., Myers, A.G., and Rees, D.C. (1993) Crystal structure of neocarzinostatin, an antitumor protein-chromophore complex. *Science* **262**, 1042–1046
22. Zein, N., Casazza, A.M., Doyle, T.W., Leet, J.E., Schroeder, D.R., Solomon, W., and Nadler, S.G. (1993) Selective proteolytic activity of the antitumor agent kedarcidin. *Proc. Natl. Acad. Sci. USA* **90**, 8009–8012
23. Heyd, B., Lerat, G., Adjadj, E., Minard, P., and Desmadril, M. (2000) Reinvestigation of the proteolytic activity of neocarzinostatin. *J. Bacteriol.* **182**, 1812–1818
24. Mohanty, S., Sieker, L.C., and Drobny, G.P. (1994) Sequential 1H NMR assignment of the complex of aponeocarzinostatin with ethidium bromide and investigation of protein-drug interactions in the chromophore binding site. *Biochemistry* **33**, 10579–10590
25. Perrin, F. (1926) Polarisation de la lumiere de fluorescence vie moyenne des molecules dans letat excite. *J. Phys. Rad.* **1**, 390–401
26. Carlson, J.C., Buhr, M.M., and Riley, J.C. (1989) Plasma membrane changes during corpus luteum regression. *Can. J. Physiol. Pharmacol.* **67**, 957–961
27. Hatch, A., Kamholz, A.E., Hawkins, K.R., Munson, M.S., Schilling, E.A., Weigl, B.H., and Yager, P.A (2001) rapid diffusion immunoassay in a T-sensor. *Nat. Biotechnol.* **19**, 461–465
28. Ou, J., Tu, H., Shan, B., Luk, A., DeBose-Boyd, R.A., Bashmakov, Y., Goldstein, J.L., and Brown, M.S. (2001) Unsaturated fatty acids inhibit transcription of the sterol regulatory element-binding protein-1c (SREBP-1c) gene by antagonizing ligand-dependent activation of the LXR. *Proc. Natl. Acad. Sci. USA* **98**, 6027–6032
29. Hsu, T.M., Law, S.M., Duan, S., Neri, B.P., and Kwok, P.Y. (2001) Genotyping single-nucleotide polymorphisms by the invader assay with dual-color fluorescence polarization detection. *Clin. Chem.* **47**, 1373–1377
30. Latif, S., Bauer-Sardina, I., Ranade, K., Livak, K.J., and Kwok, P.Y. (2001) Fluorescence polarization in homogeneous nucleic acid analysis II: 5′-nuclease assay. *Genome Res.* **11**, 436–440.
31. Nakamura, Y., Gojobori, T., and Ikemura, T. (1997) Codon usage tabulated from the international DNA sequence databases. *Nucleic. Acids Res.* **25**, 244–245
32. Crameri, R., Hemmann, S., and Blaser, K. (1996) PJuFo: a phagemid for display of cDNA libraries on phage surface suitable for selective isolation of clones expressing allergens. *Adv. Exp. Med. Biol.* **409**, 103–110
33. Crameri, R. and Blaser, K. (1996) Cloning Aspergillus fumigatus allergens by the pJuFo filamentous phage display system. *Int. Arch. Allergy Immunol.* **110**, 41–45
34. Tomioka, Y., Aihara, K., Hirose, A., Hishinuma, T., and Mizugaki, M. (1991) Detection of heat-stable delta 3,delta 2-enoyl-CoA isomerase in rat liver mitochondria and peroxisomes by immunochemical study using specific antibody. *J. Biochem.* **109**, 394–398
35. Sarkar, G. and Sommer, S. S. (1990) The "megaprimer" method of site-directed mutagenesis. *Biotechniques* **8**, 404–407
36. Smith, A.M. and Klugman, K.P. (1997) "Megaprimer" method of PCR-based mutagenesis: the concentration of megaprimer is a critical factor. *Biotechniques* **22**, 438–442
37. Peitsch, M.C. and Jongeneel, V. (1993) A 3-dimensional model for the CD40 ligand predicts that it is a compact trimer similar to the tumor necrosis factors. *Int. Immunol.* **5**, 233–238
38. Peitsch, M.C. (1995) Protein modeling by E-mail. *Bio/Technology* **13**, 658–660
39. Guex, N. and Peitsch, M.C. (1997) SWISS-MODEL and Swiss-Pdb Viewer: An environment for comparative protein modeling. *Electrophoresis* **18**, 2714–2723
40. Olmsted, J. and Kearns, D.R. (1977) Mechanism of ethidium bromide fluorescence enhancement on binding to nucleic acids. *Biochemistry* **16**, 3647–3654
41. Tanaka, T., Hirama, M., Fujita, K.-I., Imago, S., and Ishiguro, M. (1993) Solution structure of the antibiotic neocarzinostatin, a chromophore-protein complex. *J. Chem. Soc. Chem. Commun.* **15**, 1205–1207
42. Teplyakov, A., Obmolova, G., Wilson, K., and Kuromizu, K. (1993) Crystal structure of apo-neocarzinostatin at 0.15-nm resolution. *Eur. J. Biochem.* **213**, 737–741
43. Remerowski, M.L., Glaser, S.J., Sieker, L.C., Samy, T.S., and Drobny, G.P. (1990) Sequential 1H NMR assignments and secondary structure of aponeocarzinostatin in solution. *Biochemistry* **29**, 8401–8409
44. Adjadj, E., Mispelter, J., Quiniou, E., Dimicoli, J.L., Favaudon, V., and Lhoste, J.M. (1990) Proton NMR studies of apo-neocarzinostatin from Streptomyces carzinostaticus. Sequence-specific assignment and secondary structure. *Eur. J. Biochem.* **190**, 263–271
45. Takashima, H., Amiya, S., and Kobayashi, Y. (1991) Neocarzinostatin: interaction between the antitumor-active chromophore and the carrier protein. *J. Biochem.* **109**, 807–810
46. Gao, X.L. and Burkhart, W. (1991) Two- and three-dimensional proton NMR studies of apo-neocarzinostatin. *Biochemistry* **30**, 7730–7739
47. Adjadj, E., Quiniou, E., Mispelter, J., Favaudon, V., and Lhoste, J.M. (1992) The seven-stranded beta-barrel structure of apo-neocarzinostatin as compared to the immunoglobulin domain. *Biochimie* **74**, 853–858
48. Saito, K., Sato, Y., Edo, K., Akiyama-Murai, Y., Koide, Y., Ishida, N., and Mizugaki, M. (1989) Characterization of secondary structure of neocarzinostatin apoprotein. *Chem. Pharm. Bull. (Tokyo)* **37**, 3078–3082
49. Tsunoda, S., Ohizumi, I., Matsui, J., Koizumi, K., Wakai, Y., Makimoto, H., Tsutsumi, Y., Utoguchi, N., Taniguchi, K., Saito, H., Harada, N., Ohsugi, Y., and Mayumi, T. (1999) Specific binding of TES-23 antibody to tumour vascular endothelium in mice, rats and human cancer tissue: a novel drug carrier for cancer targeting therapy. *Br. J. Cancer* **81**, 1155–1161
50. Cleland, J.L. and Craik, C.S. (1996) *Protein Engineering: Principles and Practice*, Wiley-Liss, New York